The Journal of Experimental Biology **198**, 2197–2212 (1995)
Printed in Great Britain © The Company of Biologists Limited 1995

SODIUM-DEPENDENT NOREPINEPHRINE-INDUCED CURRENTS IN NOREPINEPHRINE-TRANSPORTER-TRANSFECTED HEK-293 CELLS BLOCKED BY COCAINE AND ANTIDEPRESSANTS

AURELIO GALLI, LOUIS J. DEFELICE*, BILLIE-JEANNE DUKE, KIMBERLY R. MOORE AND RANDY D. BLAKELY

Department of Anatomy and Cell Biology, Emory University School of Medicine, Atlanta GA 30322, USA

Accepted 4 July 1995

Summary

Transport of norepinephrine (NE^+) by cocaine- and antidepressant-sensitive transporters in presynaptic terminals is predicted to involve the cotransport of Na^+ and Cl^-, resulting in a net movement of charge per transport cycle. To explore the relationship between catecholamine transport and ion permeation through the NE transporter, we established a human norepinephrine transporter (hNET) cell line suitable for biochemical analysis and patch-clamp recording. Stable transfection of hNET cDNA into HEK-293 (human embryonic kidney) cells results in lines exhibiting (1) a high number of transporter copies per cell (10^6), as detected by radioligand binding and hNET-specific antibodies, (2) high-affinity, Na^+-dependent transport of NE, and (3) inhibitor sensitivities similar to those of native membranes. Whole-cell voltage-clamp of hNET-293 cells reveals NE-induced, Na^+-dependent currents blocked by antidepressants and cocaine that are absent in parental cells. In addition to NE-dependent currents, transfected cells possess an NE-independent mode of charge movement mediated by hNET. hNET antagonists without effect in non-transfected cells abolish both NE-dependent and NE-independent modes of charge movement in transfected cells. The magnitude of NE-dependent currents in these cells exceeds the expectations of simple carrier models using previous estimates of transport rates. To explain our observations, we propose that hNETs function as ion-gated ligand channels with an indefinite stoichiometry relating ion flux to NE transport. In this view, external Na^+ and NE bind to the transporter with finite affinities in a cooperative fashion. However, coupled transport may not predict the magnitude or the kinetics of the total current through the transporter. We propose instead that Na^+ gates NE transport and also the parallel inward flux of an indeterminate number of ions through a channel-like pore.

Key words: human norepinephrine transporter, stably transfected mammalian (HEK-293) cells, norepinephrine, guanethidine, desipramine, cocaine, whole-cell voltage-clamp, steady-state currents, transient currents, ion-coupled transport.

Introduction

The plasma membranes of presynaptic neurons, and certain specialized non-neuronal cells, contain transport proteins for the efficient clearance of biogenic amine neurotransmitters (Iversen, 1975; Blakely *et al*. 1991*a*,*b*; Hoffman *et al*. 1991; Kaplan, 1993; Rudnick and Clark 1993; Amara and Kuhar, 1993; Atwell *et al.* 1993; Blakely, 1993; Blakely *et al.* 1994). In particular, central and peripheral noradrenergic neurons express a catecholamine-selective transporter responsible for recovery of norepinephrine (NE) following its release (Trendelenburg, 1991; Barker and Blakely, 1995). In the periphery, where more quantitative estimates are attainable, the norepinephrine transporter (NET) may recover as much as 90 % of released neurotransmitter (Schömig *et al.* 1989, 1991). Pharmacological blockade of NETs with tricyclic antidepressants and with cocaine elevates extracellular NE concentrations and results in increased overflow of neurotransmitter from synaptic spaces (Iversen, 1975; Palij and Stamford, 1992; Gonon *et al.* 1993). As a consequence, NE may exert prolonged activation of presynaptic and postsynaptic adrenergic receptors and act more globally on extrasynaptic receptors, underscoring the important regulatory role of efficient NE clearance. This selective and efficient clearance capacity of NETs also serves as a mechanism for exogenous loading of sympathetic terminals and chromaffin cells with antihypertensive false transmitters, including guanethidine (Ross, 1987). Similarly, human neuroblastomas and pheochromocytomas that express NETs can be loaded exogenously with antitumor agents such as

*Author for correspondence.

metaiodobenzylguanidine, which is a substrate for NET (Smets *et al.* 1988). During ischemic conditions, the NET may actually drive its substrate out of sympathetic terminals in a nonvesicular mode of release, as a consequence of altered electrochemical gradients required for transport, and thereby contribute to potentially fatal arrhythmia (Schömig *et al.* 1991; see also Bernath, 1991). Indeed, cardiovascular complications following NET blockade by tricyclic antidepressants and cocaine are well recognized (Glassman *et al.* 1985; Ganguly *et al.* 1986; Clarkson *et al.* 1993.

Since the discovery of sympathetic catecholamine transport more than three decades ago (Hertting *et al.* 1961; Axelrod *et al.* 1961; Whitby and Axelrod, 1961; Axelrod, 1971), mechanistic studies of NE transport have relied exclusively upon measurements of radiolabeled substrates or the binding of radiolabeled antagonists. NETs saturate at low to sub-micromolar NE concentrations and recognize a number of structurally similar substrates, including dopamine, amphetamines and guanethidine derivatives. Studies conducted with tissue slices, synaptosomes, cultured cells and resealed membranes demonstrate that NETs require millimolar concentrations of extracellular Na^+ (Iversen and Kravitz, 1966; Bogdanski and Brodie, 1966; Sammet and Graefe, 1979; Harder and Bönisch, 1985; Bönisch and Harder, 1986) and millimolar concentrations of extracellular Cl^- (Sánchez-Armáss and Orrego, 1977; Friedrich and Bönisch, 1986; Ramamoorthy *et al.* 1993*a*,*b*). The carrier models derived from PC-12 cells and placental vesicles define a transport coupling ratio of $1Na^+$:$1Cl^-$:$1NE^+$ (Friedrich and Bönisch, 1986; Ramamoorthy *et al.* 1993*a*,*b*). Cotransport explains the influx of catecholamines against amine concentration gradients (Stein, 1986; Kanner and Schuldinger, 1987; Lauger, 1991), coupling NE movement to the energetically favorable influx of Na^+ and Cl^- down their concentration gradients at fixed stoichiometry. This model predicts that each transport cycle is electrogenic, because a net translocation of a single positive charge accompanies each cycle. However, these thermodynamic models do not describe the kinetics of charge transfer or the contributions of intermediate steps in the translocation of substrates and ions. Similarly, ion-dependence flux studies cannot reveal the true transport stoichiometry if other charge movement pathways exist that depend on the substrate but otherwise bypass the rate-limited, substrate-coupled kinetic steps (Lester *et al.* 1994).

Endogenous NET-associated charge movements have yet to be measured directly owing to the inaccessibility of noradrenergic nerve terminals and the low level of NET expression by noradrenergic cell lines. Furthermore, studies on membrane vesicles (Bönisch and Harder, 1986) have so far yielded transport rate estimates of only $2.5\,cycles\,s^{-1}$, far too small to detect NET-dependent charge movements at the assumed NET stoichiometry (Harder and Bönisch, 1985; Bönisch and Harder, 1986; Ramamoorthy *et al.* 1993*a*,*b*) even under amplified expression. Nevertheless, the currents associated with glutamate, gamma-aminobutyric acid (GABA) and serotonin uptake through presumably homologous Na^+-dependent transporters readily appear under whole-cell voltage-clamp conditions on native preparations (Brew and Atwell, 1987; Schwartz and Tachibana, 1989; Malchow and Ripps, 1990; Bruns *et al.* 1993) and on cRNA-injected *Xenopus laevis* oocytes (Clark *et al.* 1992; Mager *et al.* 1993, 1994). GABA-transporter-associated currents have also been detected in transfected mammalian cells (Risso *et al.* 1992; Laezza *et al.* 1994; Cammack *et al.* 1994; Risso *et al*. 1995). The native preparations and the heterologous expression systems suggest significantly greater transporter currents than anticipated from radiotracer flux studies.

Heterologous expression of cloned human NETs (hNETs) in transiently transfected HeLa cells has shown that a single cDNA species confers high-affinity, Na^+-dependent NE transport on non-neuronal cells. Transfected cells also have uptake inhibitor sensitivities that are similar, if not identical, to those observed in native membranes (Pacholczyk *et al.* 1991; Gu *et al.* 1994). To gain biophysical insight into the nature of cocaine- and antidepressant-dependent catecholamine transport, we have established hNET-expressing cell lines suitable for biochemical analyses, radiolabled flux studies and patch-clamp recording techniques. Here we document the expression and the functional characteristics of hNET stably transfected in HEK-293 (human embryonic kidney) cells using immunological and radiometric techniques. Electrophysiological measurements in these cells reveal Na^+-dependent, cocaine- and antidepressant-sensitive, NE-induced currents as implied from radiolabeled flux experiments. Currents have Michaelis–Menten dependence on extracellular concentrations of NE and Na^+. NE-independent modes of charge transfer also correlate with the expression of hNET. NET antagonists that lack effects on non-transfected cells abolish the NE-independent modes of charge movement in transfected cells. The magnitude and kinetics of the NE-dependent and the NE-independent currents require re-evaluation of previous carrier models of transport and earlier estimates of transport rates. Our data conform to expectations for an ion-gated ligand channel where ions (Na^+ and Cl^-) and the substrate (NE^+) bind and are cotransported with fixed stoichiometry, but where the substrate-gated charge flux may generate an additional current of indeterminate stoichiometry.

Materials and methods

Stable cell lines

An XhoI/XbaI fragment containing complete hNET cDNA was released from pBluescript SKII- (Pacholczyk *et al.* 1991) and subcloned into XhoI/XbaI-digested pcDNA3 (Invitrogen). This places hNET expression under control of the CMV promoter as well as the T7 RNA polymerase promoter. We validated the new construct by demonstrating functional hNET expression in transiently transfected HeLa cells using vaccinia–T7 expression (Fuerst *et al.* 1986; Blakely *et al.* 1991*b*) prior to stable transfection. To generate stably transfected cells, hNET/pcDNA3 was transfected by Lipofectin (Life Technologies) into HEK-293 cells at 50–60 %

confluency. The medium was Dulbecco's Modified Eagle Medium with 10 % heat-inactivated fetal bovine serum, 100 μg ml^{-1} penicillin and 100 i.u. ml^{-1} streptomycin. After 3 days, parental and transfected cells were switched to a medium containing 250 μg ml^{-1} geneticin (G418), and the resistant colonies were isolated from transfected plates 1 week later using sterile clone rings. Individual cells were used to generate clonal lines. Multiple lines tested positive for desipramine-sensitive [^{3}H]NE uptake and transporter-associated currents. Clonal line 293-hNET-#3 (termed 293-hNET cells) was used in all experiments reported here.

Transport assays

293-hNET cells were plated at a density of approximately 50×10^3 cells per well on poly-L-lysine-coated (1 mg ml^{-1}), 24-well tissue culture plates 1 day prior to experiments. On the day of experiments, the medium was removed by aspiration. Cells were then pre-incubated for 10 min in Krebs–Ringer's–Hepes (KRH) medium with or without antagonists (in mmol l^{-1}): 130 NaCl, 1.3 KCl, 2.2 $CaCl_2$, 1.2 $MgSO_4$, 1.2 KH_2PO_4, 10 Hepes, 1.8 g l^{-1} dextrose, pH 7.4 at 37 °C). Transport assays (10 min at 37 °C) were initiated by adding [2,5,6,3-^{3}H]norepinephrine ([^{3}H]NE, Dupont/NEN), 50 nmol l^{-1} final concentration in a final assay volume of 1 ml. To block spontaneous oxidation and metabolism of NE by monoamine oxidases and catechol-*O*-methyl transferases, [^{3}H]NE cocktails were diluted in KRH supplemented to achieve 100 μmol l^{-1} L-ascorbate, 100 μmol l^{-1} pargyline and 10 μmol l^{-1} U-0521 (UpJohn; catechol-*O*-methyltransferase inhibitor) final assay concentrations. Competitors such as guanethidine (GU) and unlabeled NE were added at the same time as the [^{3}H]NE. Assays were terminated by medium aspiration followed by two rapid 1 ml washes at room temperature in KRH and extraction of incorporated radioactivity with 500 μl of 1 % sodium dodecylsulfate (SDS). Accumulated radioactivity was quantified by liquid scintillation spectrometry. Nonspecific [^{3}H]NE transport was determined in parallel assays conducted in the presence of 1 μmol l^{-1} desipramine or 10 μmol l^{-1} nomifensine (for desipramine inhibition experiments). This background flux was subtracted from flux data obtained in the absence of inhibitors. The data represent mean ± S.E.M. of experiments performed in triplicate.

Membrane binding assays

Total cell membranes were prepared from transfected cells grown to confluence in 150 mm tissue culture dishes. Cells were scraped into standard medium and pelleted at 1600 ***g***. The medium was discarded and the pellet resuspended in 5 ml per plate of ice-cold binding buffer (100 mmol l^{-1} NaCl, 50 mmol l^{-1} Tris, pH 7.4 at room temperature) by trituration, and the cells were repelleted at 20 000 ***g***. Supernatant was discarded and cells were resuspended in binding buffer and homogenized with a polytron (Brinkman) at 25 000 revs min^{-1} for 5 s. Centrifugation, resuspension and homogenization were repeated and a sample of suspension was used for Bradford protein determination (BioRad). Samples of membrane suspensions were frozen at −80 °C prior to use. Typical yields were about 100 μg membrane protein per 10^6 cells. hNET density was assessed with the radioligand [^{125}I]RTI-55 [3β-(4-iodophenyl)-tropan-2β-carboxylic acid methylester tartrate; Dupont/NEN], which has previously been demonstrated to bind with nanomolar affinity to hNET expressed in LLC-PK_1 cells (Gu *et al.* 1994; Melikian *et al.* 1994). Initial studies with 293-hNET cell membranes demonstrated linearity of specific binding up to 10 μg protein per tube; subsequent binding assays utilized 10 μg per tube. Assays performed in duplicate were initiated with 0.1 nmol l^{-1} [^{125}I]RTI-55 in increasing concentrations of unlabeled RTI-55. Assays were terminated by rapid filtration over GF/B glass-fiber filters soaked in 0.5 % polyethylineimine using an automated cell harvester (Brandel) followed by three rapid 5 ml washes in ice-cold binding buffer. Bound radioactivity was measured by gamma emission spectrometry. Nonspecific binding was determined from assay tubes containing 1 μmol l^{-1} desipramine incubated in parallel; this background binding was subtracted from the data in the absence of desipramine to yield specific binding.

hNET immunoblotting

Affinity-purified N430 antibody (0.5 μg ml^{-1}, Melikian *et al.* 1994) from whole 293-hNET cell extracts was used to validate hNET protein expression (25 μg per lane). As a positive control, extracts (30 μg per lane) of the previously characterized LLC-NET stable cell line (Gu *et al.* 1994; Melikian *et al.* 1994) were blotted in parallel. As negative controls, parallel blots were performed with pre-immune serum (6 μg ml^{-1}) or with N430 antibody using parental HEK-293 cell extracts. Bound primary antibodies were detected using horseradish-peroxidase-conjugated goat anti-rabbit antibody (1:3000, BioRad) and immunoreactive bands were detected by enhanced chemiluminescence (Amersham) on X-ray film (Kodak X-AR).

Electrophysiology

Stably transfected HEK-293 cells have advantages over transiently transfected HeLa cells (Risso *et al.* 1992; Risso *et al.* 1995). They express transporters more uniformly, have more negative resting potentials (−30 to −50 mV) and form tighter seals (greater than 20 GΩ) for whole-cell voltage-clamp than transiently transfected HeLa cells from our previous experimental model (Risso *et al.* 1992). Prior to electrical recording, parental or stably transfected cells were plated at a density of 10^5 per 35 mm culture dish and attached cells were washed three times with bath solution at room temperature. Except for the extracellular Na^+ replacement experiments (Fig. 5B), all data were obtained under temperature control at 37 °C. The normal bath contained (in mmol l^{-1}): 130 NaCl, 1.3 KCl, 1.3 KH_2PO_4, 0.5 $MgSO_4$, 1.5 $CaCl_2$, 10 Hepes and 34 dextrose. The solution was adjusted to pH 7.35 and 300 mosmol l^{-1} with 1 mol l^{-1} NaOH and dextrose. In the extracellular Na^+ replacement experiments, LiCl or TrisCl replaced NaCl. Pipette solutions for the whole-cell recording contained (in mmol l^{-1}): 130 KCl, 0.1 $CaCl_2$, 2 $MgCl_2$, 1.1 EGTA, 10 Hepes and 30 dextrose, adjusted to pH 7.35 and

270 mosmol l^{-1}. Free Ca^{2+} in the pipette was 0.1 μmol l^{-1}. To confirm the transporter specificity of the norepinephrine (NE)- and guanethidine (GU)-induced currents, we recorded in the absence and presence of the specific NE uptake inhibitor desipramine (DS) or the general monoamine uptake inhibitor cocaine. Solutions were exchanged by a gravity pump at a rate of 1 ml min^{-1} for the Na^+-dependent experiments (effective temperature 33 °C). Otherwise, we added NE, GU and DS to a 3.5 ml bath at 100× concentrations to obtain the final concentrations. To prevent oxidation of NE, solutions contained 100 μmol l^{-1} pargyline and 100 μmol l^{-1} ascorbic acid. Patch electrodes (5 MΩ) were pulled from borosilicate glass (Corning 7052) with a programmable puller (Sachs-Flaming, PC-84). An Axopatch 200A amplifier band-limited at 5000 Hz was used to measure current. Series conductance was 0.1 μS or greater, and cell capacitance was 25–80 pF, implying a surface area of 2500–8000 μm^2. Different expression levels from cell to cell prevented normalization of the current to surface area. To compare cells, we normalized the currents to the maximum value for a given protocol. Voltage steps ranged from −140 to 0 mV and lasted 500 ms. Test pulses were separated by −40 mV holding potentials for either 1 s or 5 s. Values for steady-state currents were taken between 400 and 500 ms after the step. Data were stored digitally on a video recorder and analyzed on a Nicolet 4094 oscilloscope and an IBM-AT computer using instrumentation and programs written by W. N. Goolsby (information available on request).

Results

Transfected cells express hNET protein and bind a cocaine analogue with high affinity

Multiple colonies of hNET cDNA-transfected HEK-293 cells were isolated after antibiotic (G418) selection and assayed for desipramine-sensitive [^{3}H]NE transport. One of these lines (293-hNET cells) was expanded and analyzed for expression of NET by immunoblotting, radioligand binding and radiolabeled flux studies. As shown in Fig. 1A, 293-hNET cells express an 80 kDa immunoreactive species detected by the affinity-purified antipeptide NET antibody N430 cells (Melikian *et al.* 1994). The 80 kDa species was absent from the parental line as well as from lanes blotted with pre-immune serum. The protein detected in 293-hNET cells appears as a broad band consistent with micro-heterogeneity in glycosylation. The hNET protein in HEK-293 cells migrates similarly to the most mature *N*-glycosylated hNET protein in previously characterized LLC-NET cells (Melikian *et al.* 1994). To obtain quantitative information on expression of hNET, we prepared total cell membrane from 293-hNET cells and assayed the equilibrium binding of the high-affinity cocaine analogue [^{125}I]RTI-55 (Fig. 1B). For binding assay data, we used a nonlinear least-squares fit. Fitting of saturation data was achieved utilizing a generalized saturation equation:

$$B = B_{max}\,[L]^n(K_D{}^n + [L]^n)\,, \qquad (1)$$

where B is the number of moles bound, K_D is the dissociation

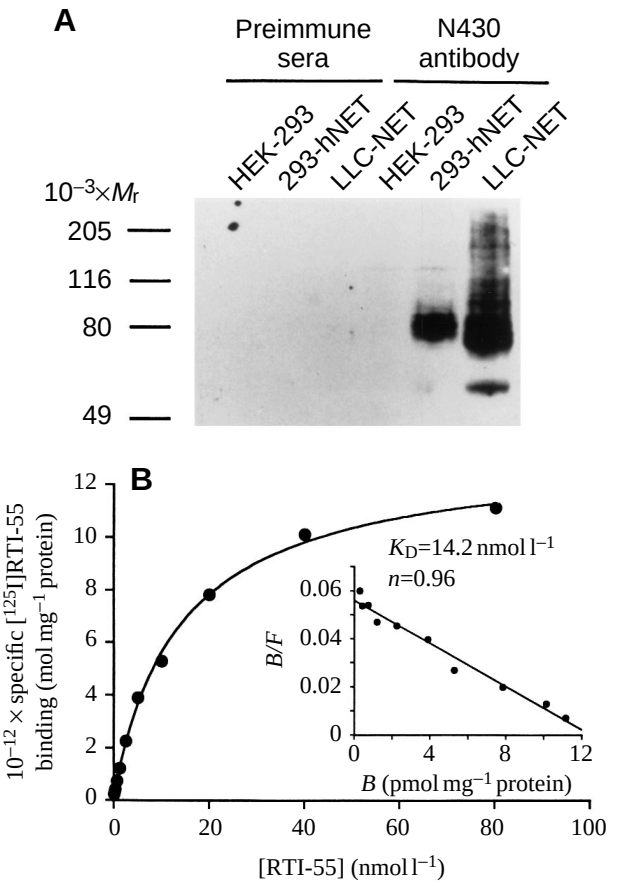

Fig. 1. Expression of hNET in stably transfected HEK-293 cells. (A) Immunoblot of hNET protein expressed in HEK-293 cells. Membranes were prepared as described in Materials and methods and subjected to SDS–PAGE (8 %) prior to immunoblot analysis with either preimmune sera (6 μg ml $^{-1}$) or affinity-purified N430 antibody (Ab) (0.5 μg ml $^{-1}$). In each lane, 25 μg of protein from whole-cell lysates of parental HEK-293 cells or transfected 293-hNET cells was electrophoresed and blotted, except for the LLC-NET lanes where 30 μg of protein was used. The numbers to the left of the blot indicate the migration of molecular mass markers electrophoresed in parallel. (B) Equilibrium binding of [^{125}I]RTI-55 to 293-hNET membranes. Membranes, prepared as described in Materials and methods, were incubated with varying concentrations of RTI-55 and a constant concentration (0.1 nmol l^{-1}) of [^{125}I]RTI-55 to obtain a saturation profile of antagonist binding to transfected hNET. The inset shows a linear fit to a Rosenthal transformation of the binding data, consistent with a single population of non-interacting [^{125}I]RTI-55 binding sites with a K_D of 14.2±1.6 nmol l^{-1}. B/F is the bound/free fraction. B_{max} values obtained were 13.1±0.6 pmol mg^{-1} protein which, on the basis of membrane recovery, converts to approximately 9×10^5 sites per cell.

constant, n is the Hill coefficient and L is the binding ligand [^{125}I]RTI-55. Fig. 1B demonstrates that [^{125}I]RTI-55 binds saturably to 293-hNET cell membranes with a K_D of 14.2±1.6 nmol l^{-1}, a Hill coefficient n of 0.96±0.1 and a B_{max} of 13.1±0.6 pmol mg^{-1} protein (means ± S.E.M., N=3). These data are consistent with a single population of non-interacting transporter sites labeled by [^{125}I]RTI-55. A conversion of B_{max}

based on protein yield per cell gives an average value of 9×10^5 [^{125}I]RTI-55 binding sites per 293-hNET cell.

Transfected cells transport norepinephrine: antagonists and competitors inhibit this uptake

To explore the functional properties of NE transport in 293-hNET cells, we performed saturation kinetic analyses of [^{3}H]NE transport combined with inhibitor studies at low [^{3}H]NE concentrations. Nonlinear least-squares curve-fitting (Kaleidagraph) of saturation data was achieved for the generalized Michaelis–Menten equation:

$$V = V_{max}[S]^n/(K_m^n + [S]^n), \quad (2)$$

where V is the velocity of uptake, [S] is the substrate concentration, K_m is the Michaelis–Menten constant and n is the Hill coefficient. [^{3}H]NE transport obeys saturable kinetics with a K_m of 420±38 nmol l^{-1}, a Hill coefficient of 1.3±0.1 and a V_{max} of $5.2\times10^{-17}\pm0.1\times10^{-17}$ mol cell^{-1} min^{-1} (Fig. 2A). If all hNET sites detected by [^{125}I]RTI-55 binding contribute to transport of [^{3}H]NE, the ratio V_{max}/B_{max} gives an estimate of cycle rate equal to 1.7 s^{-1} at 37 °C. [^{3}H]NE transport in 293-hNET cells was sensitive to compounds known to inhibit [^{3}H]NE uptake specifically in native tissues. For the inhibition curves (Fig. 2B), the IC_{50} values (the concentration of inhibitor causing 50 % inhibition) were determined from fits of the logistic equation with conversion to K_I values according to Cheng and Prusoff (1973). The NET-selective antagonist nomifensine inhibits [^{3}H]NE uptake with a K_I of 4.5 nmol l^{-1}. The secondary amine tricyclic antidepressant desipramine (DS) was an order of magnitude more potent (K_I=2.9 nmol l^{-1}) than its tertiary amine derivative imipramine (K_I= 35.2 nmol l^{-1}), similar to observations from transiently transfected HeLa cells (Pacholczyk *et al.* 1991). Cocaine, which is a non-selective biogenic amine transporter antagonist, blocked specific [^{3}H]NE transport with a K_I of 370 nmol l^{-1}. Finally, the false transmitter guanethidine, a known substrate for NET (Ross, 1987), inhibited [^{3}H]NE uptake with a K_I of 6.7 μmol l^{-1}. All inhibition profiles conformed to fits with Hill coefficients near unity.

Norepinephrine induces an inward current in 293-hNET cells that is blocked by desipramine

Fig. 3 shows data from whole-cell voltage-clamped parental and transfected cells. Holding potential was −40 mV and test potentials were −80 or −120 mV. Raw data at 37 °C are neither leak-subtracted nor capacity-compensated. Fig. 3A,B demonstrates that NE and DS have no effect on background currents in the parental cell line. The fast transient current and

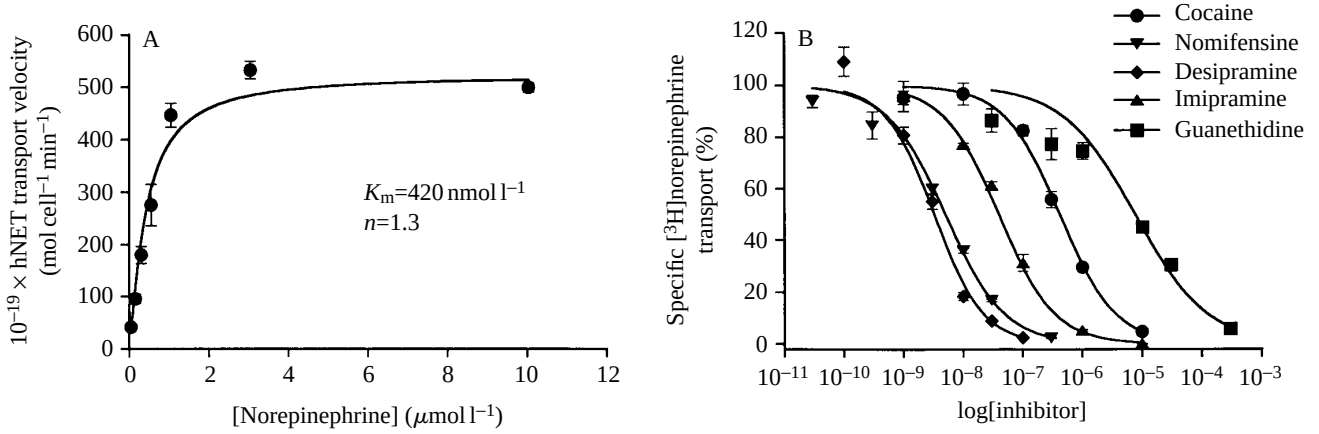

Fig. 2. Kinetics and inhibitor insensitivity of [^{3}H]norepinephrine (NE) transport in 293-hNET cells. (A) Kinetics of [^{3}H]NE uptake in 293-hNET cells. [Substrate]/velocity profiles were derived from transport studies conducted as described in Materials and methods with varying concentrations of L-NE and a fixed concentration (50 nmol l^{-1}) of [^{3}H]NE. Parallel incubations with 1 μmol l^{-1} desipramine were used to assess the level of nonspecific transport, and these values were subtracted from our raw data to yield specific NE transport. Velocity data were fitted by nonlinear least-squares analysis to the generalized Michaelis–Menton formulation: $V=V_{max}[NE]^n/([NE]^n+K_m^n)$, where [NE] is the total external NE concentration, K_m is the concentration of NE at $0.5V_{max}$ and n is the Hill coefficient. From these data, we extract K_m=420±38 nmol l^{-1}, $V_{max}=5.2\times10^{-17}\pm0.1\times10^{-17}$ mol cell^{-1} min^{-1} and a Hill coefficient of 1.3±0.1. These data were obtained 10 min after adding radiolabeled NE to the bath. V_{max} values are constant to within ±10 % between 10 s and 10 min. Non-specific uptake in mock transfected cells and in parental cells was less than 5 % of the total blockable uptake. Values are means ± S.E.M., N=3. (B) Inhibitor sensitivity of [^{3}H]NE transport in 293-hNET cells. Inhibitor potencies were estimated in [^{3}H]NE (50 nmol l^{-1}) transport assays conducted with various concentrations (in mol l^{-1}) of monoamine transporter inhibitors and substrates. Parallel incubations with 1 μmol l^{-1} desipramine were used to assess the level of nonspecific transport, except in the desipramine inhibition experiments, where 10 μmol l^{-1} nomifensine was used. Non-specific values were subtracted from our raw data to yield specific NE transport and the data are expressed as a percentage of NE accumulated in the absence of antagonist. Data were fitted to a two-parameter logistic expression: percentage of specific NE transport remaining=$100/\{1+(IC_{50}/[I])^n\}$, where IC_{50} is the concentration of competitor giving 50 % inhibition, [I] is the inhibitor concentration and n is the slope (Hill coefficient). IC_{50} values were converted to K_I values using the Cheng–Prusoff (1973) correction for substrate concentration. This analysis yielded K_I values as follows: desipramine, 2.9±0.2 nmol l^{-1}; nomifensine, 4.5±0.2 nmol l^{-1}; imipramine, 35.2±1.0 nmol l^{-1}; cocaine, 370±20 nmol l^{-1} and guanethidine, 6.7±0.2 μmol l^{-1}. Slope values were all at or close (±0.2) to unity. Values are means ± S.E.M., N=3.

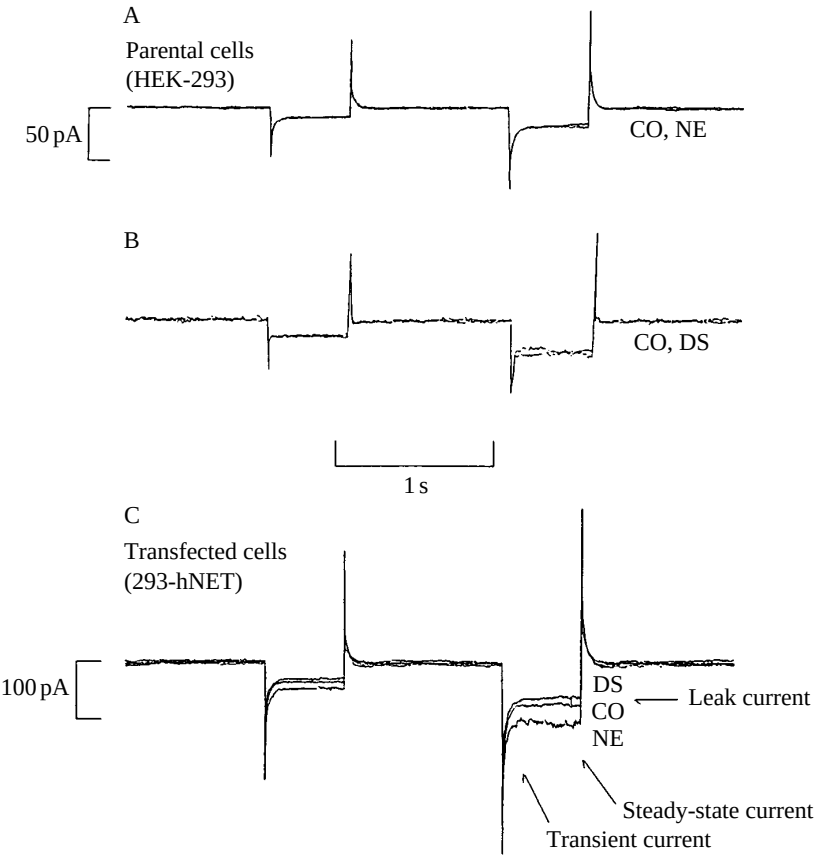

Fig. 3. Norepinephrine (NE) induces an inward current in 293-hNET cells and desipramine (DS) blocks this current. In this figure, CO represents the control current (no NE, no DS), NE is the current after adding substrate (30 μmol l^{-1} NE, no DS) and DS is the current after adding inhibitor (30 μmol l^{-1} NE and 2 μmol l^{-1} DS). All traces represent raw data without leak subtraction or capacity compensation. (A) Parental cells (HEK-293). Control currents in parental cells before (CO and after (NE) adding 30 μmol l^{-1}M NE to the bath recorded in standard electrophysiological solutions at 37 °C. Voltage steps ranged from a holding potential of −40 mV (1 s) to a test potential of –80 or −120 mV (500 ms). (B) Parental cells (HEK-293). Control currents in parental cells before (CO) and after (DS) adding 2 μmol l^{-1} DS to the bath. The same voltage protocol as in A was applied. (C) Transfected cells (293-hNET). The same voltage protocol as in A was applied to stably transfected 293-hNET cells. The substrate-dependent current is defined as (NE − CO) or (NE − DS), and the substrate-independent current is (CO − DS). The NE-induced currents are abolished in DS; however, in most experiments 2 μmol l^{-1} DS reduces the current below the control level. Steady-state currents (CO − DS) are called leak currents. NE and DS also alter the currents that occur immediately after the voltage step, called transient currents.

the steady-state current following the voltage step are virtually the same in parental cells with or without NE or DS (*N*=6 cells). Fig. 3C shows that bath-applied NE generates an inward current in transfected cells. This current is evident at −120 mV but is also present at −40 and −80 mV. The data demonstrate that NE increases the steady-state component of the current and alters the transient (pre-steady-state) component. Both are blocked after adding DS. A consistent observation is that DS reduces NE-induced steady-state current below the control current in transfected cells only. Thus, we associate the leak current (CO − DS) with the presence of hNET proteins in the cell membrane. We analyze the leak and transient currents below (see Figs 7–9).

We considered the possibility that the NE-induced current was a direct result of NET-mediated transport or a secondary effect caused by the activation of other electrogenic pumps by Na^+. Na^+ entry could stimulate the Na^+/K^+ pump and the Na^+/Ca^{2+} exchanger, and the NE-induced current might reflect the activity of these transporters. For Na^+/K^+-ATPase, Na^+ entry would stimulate an outward current at −100 mV (Gadsby and Nakao, 1989), which is in the opposite direction to the observed current. Furthermore, 100 μmol l^{-1} ouabain has no effect the NE-induced current (data not shown), and the pipette solution used in our experiments contains no ATP. Activation of Na^+/Ca^{2+} exchangers would stimulate an inward current at −100 mV (Weir and Beuckelmann, 1989), the same direction as the current that we observe. However, 5 mmol l^{-1} Ni^+ has no effect on the control current in parental cells or on the NE-induced current in transfected cells (data not shown). Thus, it is unlikely that the NE-induced currents are related either to Na^+/K^+-ATPase activity or to Na^+/Ca^{2+} exchange.

A second NET substrate induces an inward current: current/voltage curves for norepinephrine and guanethidine

To investigate further whether the induced currents are associated with the hNET protein, we used a well-known alternative substrate for NETs. Guanethidine, used as an antihypertensive false transmitter (Ross, 1987), competitively inhibits NE transport (Fig. 2B) and is transported by NETs. Using GU as a substrate has the benefit that there is little or no activity at adrenergic receptors, reducing the possibility that the induced current is receptor-mediated. Furthermore, GU has a potentially greater charge (+3e$^-$) than NE (+1e$^-$) at the pH of our experiments (7.4) and offers the possibility of larger currents. We found that GU-induced currents have similar kinetics to NE-induced currents but are on average over twice the size. In Fig. 4 we compare current–voltage *I*(*V*) curves for NE-induced and GU-induced inward currents in parallel dishes of transfected cells. Voltage was stepped from −40 mV to −140 mV. Average current was measured between 400 and 500 ms during the test pulse. *I*(*V*) relationships were defined by the steady-state current in the presence and absence of norepinephrine (NE − CO) or guanethidine (GU − CO). We

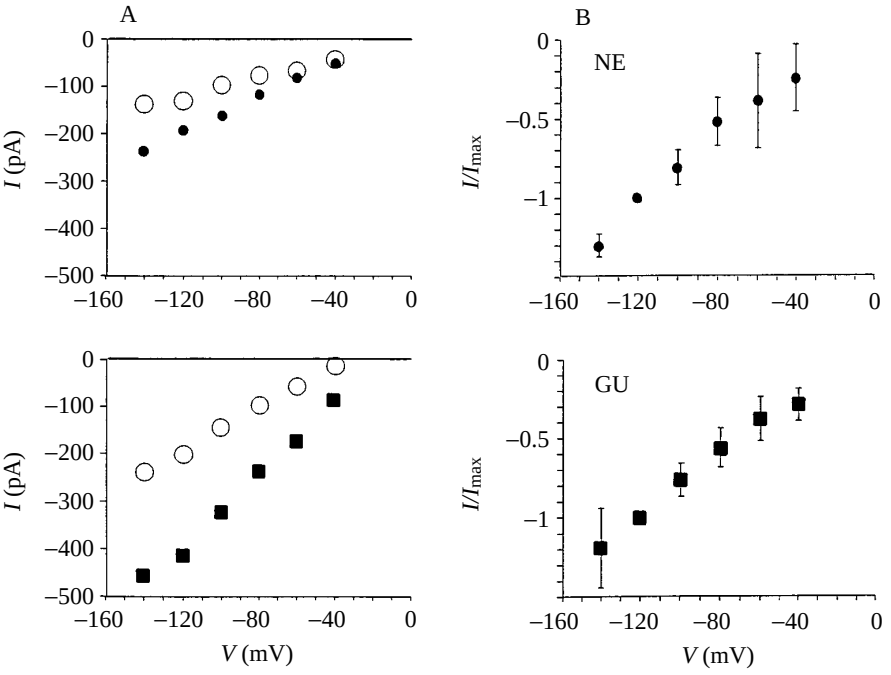

Fig. 4. Steady-state *I*(*V*) curves for NE- and guanethidine (GU)-induced currents in 293-hNET cells. (A) Raw data for NE (top panel) and GU (bottom panel). The background *I*(*V*) curves (large open circles) were obtained under control conditions (no substrate, no inhibitor). Substrate-induced *I*/(*V*) curves (filled circles or squares) are defined as the difference between background current and NE- or GU-induced, steady-state inward currents at each voltage. Substrate concentration in both cases was 30 μmol l^{-1}. The holding potential was −40 mV for 1 s between steps. The steps to the test voltage lasted 500 ms. Steady-state current was defined as the average current during 400–500 ms. (B) Subtracted cumulative data for NE-induced and GU-induced steady-state currents. The difference currents (NE − CO) and (GU − CO) illustrated in A are plotted against the test voltage (five cells each for NE and GU). Data were normalized at −120 mV. Substrate concentration is 30 μmol l^{-1} in both cases. Values are means ± S.E.M., *N*=3.

used a fixed saturating concentration of substrate (see Fig. 5). Fig. 4A shows two experiments from different cells, and Fig. 4B shows the normalized cumulative data. NE- and GU-induced currents have approximately the same steady-state voltage-dependence. Like the NE-induced currents, the GU-induced currents are blocked by DS and cocaine with similar kinetics (see Fig. 6). The GU-induced currents are 2.4 times larger than the NE-induced currents; at −120 mV they are nominally −50 pA for NE and −120 pA for GU (see Fig. 5).

Induced currents depend on norepinephrine, guanethidine and Na$^+$ concentrations

To characterize the concentration-dependence of the currents, the level of amine substrates in the bath was increased incrementally from 0 to 30 μmol l^{-1}. Voltage was stepped from −40 to −120 mV. At each new concentration, we waited 10 steps to obtain the steady-state current. [Na$^+$] was constant at 130 mmol l^{-1} and data from four cells were normalized at −120 mV and 30 μmol l^{-1} NE. The data shown in Fig. 5A were fitted by nonlinear regression to the equation:

$$I = I_{max}[NE]^n/(K_m^n + [NE]^n), \quad (3)$$

with K_m=600±40 nmol l^{-1} and n=1.02±0.06 (three cells for each data point). If all hNET sites detected by [^{125}I]RTI-55 binding contribute to the current, $I_{NE,max}/B_{max}$ gives an estimate of cycle time. Assuming fixed stoichiometry and a net charge of 1, cycle rate is 340 s^{-1}. Fig. 5B shows the dependence of NE-induced current on external [Na$^+$]. [NE] was constant at a saturating concentration (30 μmol l^{-1}) and [Na$^+$] was increased from 2.5 to 130 mmol l^{-1}. LiCl was substituted for NaCl to maintain osmolarity. 2.5 mmol l^{-1} Na$^+$ (rather than 0 mmol l^{-1} Na$^+$) is the initial concentration because 2.5 mmol l^{-1} Na$^+$ + 30 μmol l^{-1} NE results in a current approximately equal to the control current (130 mmol l^{-1} Na$^+$ + 0 mmol l^{-1} NE). Fig. 5B plots (*x*NaCl + *y*LiCl + 30 μmol l^{-1} NE) − (2.5 mmol l^{-1} NaCl + 127.5 mmol l^{-1} LiCl + 30 μmol l^{-1} NE) as a measure of Na$^+$-dependent, NE-induced current. We waited 10 voltage steps for the current to reach a steady state. These data were fitted to:

$$I = I_{max}[Na^+]^n/(K_m^n + [Na^+]^n), \quad (4)$$

which gave n=1.1±0.2 and K_m=15.0±3.0 mmol l^{-1} (three cells, normalized at −120 mV and 130 mmol l^{-1} Na$^+$). Fig. 5C shows the results for GU using the same procedure. These data were fitted to:

$$I = I_{max}[GU]^n/(K_m^n + [GU]^n), \quad (5)$$

with n=1.1±0.14 and K_m=2.4±0.27 μmol l^{-1} (four cells, normalized at −120 mV and 30 μmol l^{-1} GU). If all sites detected by [^{125}I]RTI-55 contribute to current, $I_{GU,max}/B_{max}$ gives an estimate of cycle rate; assuming three charges per cycle, gives 270 s^{-1}. The Na$^+$-dependence of GU-induced currents was similar to that of NE-induced currents; the dose–response curve for Na$^+$ gave K_m=11.5±1.5 mmol l^{-1}, n=1.39±0.2 (data not shown).

Desipramine and cocaine inhibit the norepinephrine-induced current

In Fig. 6 we present data where we evoked a current by constant exposure to 15 μmol l^{-1} NE and 130 mmol l^{-1} Na$^+$. Cells were held at −40 mV and repeatedly stimulated at 5 s intervals to −120 mV while the concentration of the inhibitor was increased incrementally. At each concentration, the current was allowed to reach a new steady state and then plotted against inhibitor concentration. Inhibition curves take 3–4 min to complete; in the absence of an inhibitor, repeated

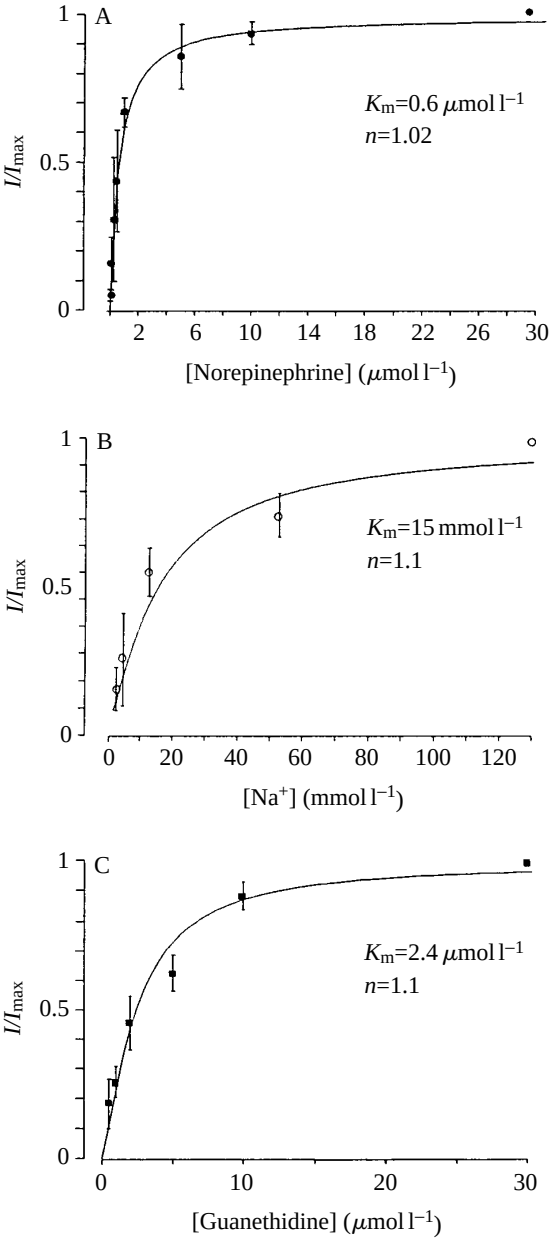

Fig. 5. Substrate- and Na^+-concentration-dependence of hNET currents in 293-hNET cells. (A) NE-induced inward current in 293-hNET cells. Each data point is derived from repeated steps (N=5) to the test potential of −120 mV (400–500 ms) from a holding potential of −40 mV (1 s). Only the difference currents (NE − CO) are shown (average for three cells). External NE concentration was varied by adding 100-fold concentrations of NE serially and incrementally to the external bath. Concentrations of Na^+ (130 mmol l^{-1}) and other ions were held constant. The data were fitted to the equation: $I=I_{max}[NE]^n/(K_m^n+[NE]^n)$ with two free parameters: K_m= 0.60±0.04 μmol l^{-1} and n=1.02±0.06. I_{max} was normalized for each cell at 30 μmol l^{-1} NE. I_{max}=48.8±19.3 pA (N=5). (B) [Na^+]-dependence of NE-induced inward current. Only the steady-state portions of the difference currents (NE − CO) were used (V=−120 mV, [NE]=30 μmol l^{-1}; average four cells). External Na^+ concentration was varied by replacing external NaCl with LiCl under constant perfusion to maintain osmolarity. The data were fitted to: $I=I_{max}[Na^+]^n/(K_m^n+[Na^+]^n)$ with two free parameters: K_m= 15.0±3.0 mmol l^{-1} and n=1.1±0.2. I_{max} was normalized for each cell at 130 mmol l^{-1} Na^+. Each point is (xNaCl+yLiCl)− (2.5NaCl+127.5LiCl). (C) GU-induced inward current. Only the steady-state portion of the difference currents (GU − CO) were used (V=−120 mV, [GU]=30 μmol l^{-1}; average three cells). The data were fitted to the equation: $I=I_{max}[GU]^n/(K_m^n+[GU]^n)$ with two free parameters: K_m=2.4±0.27 μmol l^{-1} and n=1.1±0.14. I_{max} was normalized for each cell at 30 μmol l^{-1} GU. I_{max}=117±36.0 pA (N=5). Values are means ± S.E.M., N=3.

steps show no decline in NE-induced currents over a comparable period. The maximum current in the absence of inhibitor was used to normalize each experiment. At 1 μmol l^{-1} DS, inhibition of the current is essentially complete. On average, DS reduces the current slightly below the control current (no NE, no inhibitor). We therefore fitted these data to a modified inhibition equation:

$$I = I_{min} + (I_{max} - I_{min})IC_{50}^n/(IC_{50}^n + [I]^n), \quad (6)$$

where [I] stands for the external concentration of DS or cocaine. For DS, IC_{50}=68±8 nmol l^{-1} and n=0.99±0.08 (four cells). I_{min} is the current in 30 μmol l^{-1} DS. In similar experiments with cocaine (Fig. 6B), inhibition of the current was complete in 10 μmol l^{-1}. At higher concentrations, the reduction below baseline was more dramatic than for DS. For cocaine, n=0.9±0.1 and IC_{50}=1.71±0.2 μmol l^{-1} (four cells, I_{min} at 100 μmol l^{-1} cocaine). The IC_{50} values, which were obtained at −120 mV, were converted to K_I=1.92 nmol l^{-1} for DS and to K_I=65 nmol l^{-1} for cocaine according to Cheng and Prusoff (1973).

Effect of guanethidine and desipramine on the pre-steady-state transient current

We have shown that NE and GU induce a Na^+-dependent, DS-sensitive steady-state current in 293-hNET cells. During the course of these experiments, we noticed that the pre-steady-state transient currents after a step in voltage were consistently larger in transfected cells. To explore the relationship between pre-steady-state and steady-state currents, we developed a subtraction procedure to isolate transporter transient currents. All cells have a membrane capacitance and integral membrane charge that contribute to the pre-steady-state current. For the same stimulus, these transient currents will vary from cell to cell. To eliminate unwanted transients, we subtracted test from control traces for the same cell. We did not compensate electronically; instead, we relied on the capacitance component and other components unrelated to hNET being the same in the presence or absence of NET-specific agents. We chose GU as a substrate to provide large signals. The subtraction procedures (Fig. 7) are thus: (GU − CO), (CO − DS) and (GU − DS). We used the same procedures on parental cells (Fig. 7B,C right-hand panels), and virtually no transients were visible following voltage steps. Thus, the subtraction effectively removed non-transporter-associated transients from 293-hNET cells. Hereafter the term ‘transient’ refers only to transporter-

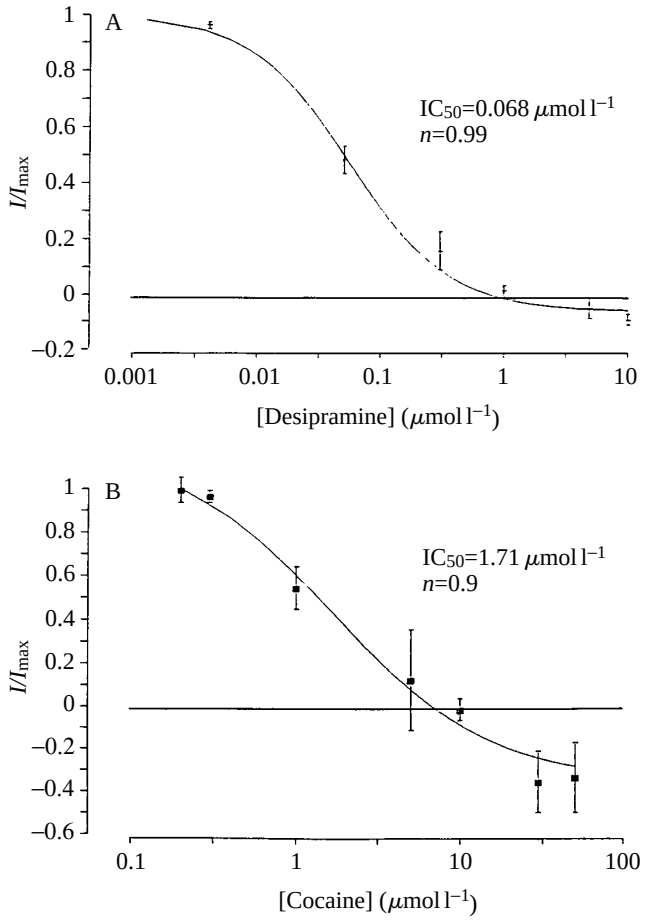

Fig. 6. Desipramine (DS) and cocaine blockade of NE-induced currents in 293-hNET cells. (A) Inhibition of NE-induced current by DS. Normalized inward currents (voltage held at −40 mV and repeatedly stepped to −120 mV for 500 ms, four cells) as a function of external [DS]. In each data set, the current was evoked by 15 μmol l^{-1} NE and measured at increasing concentrations of DS. It took 3–4 min to obtain one graph. Data were fitted to the equation (where [I] is the concentration of external DS): $I=I_{min}+(I_{max}-I_{min})IC_{50}^{n}/(IC_{50}^{n}+[I]^{n})$, with two free parameters: IC_{50}=68±8 nmol l^{-1} and n=0.99±0.08. Currents were normalized for each cell to I_{max}, the maximum NE-induced current in the absence of DS. The minimum current I_{min} refers to the current at 10 μmol l^{-1} DS at −120 mV. (B) Inhibition of NE-induced current by cocaine. Normalized data (voltage held at −40 mV and repeatedly stepped to −120 mV for 500 ms, four cells) as a function of external cocaine concentration. In each data set, the current was evoked by 15 μmol l^{-1} NE and measured at various concentrations of cocaine. Data were fitted to the same equation as in A (where [I] is the concentration of external cocaine) with two free parameters: IC_{50}=1.71±0.2 μmol l^{-1} and n=0.9±0.1. Currents were normalized for each cell to I_{max}, the maximum NE-induced current in the absence of cocaine. The minimum current I_{min} refers to the current at 100 μmol l^{-1} cocaine at −120 mV. The IC_{50} values were obtained at −120 mV and were converted to K_I=1.92 nmol l^{-1} for DS and K_I=65 nmol l^{-1} for cocaine according to Cheng and Prusoff (1973). Values are means ± S.E.M., N=3.

associated currents ($I_{transient}$) as determined by these procedures.

For the purposes of analysis, we assume that the hNET-associated current is the sum of the transient current and the steady-state current. Experimentally we have defined two steady-state currents, a substrate-induced component ($I_{substrate}$) stimulated by NE or GU (Fig. 5) and a leak component (I_{leak}) revealed by DS or cocaine (Figs 3, 6). In Fig. 3, DS reduced the current below control levels; however, NE was still present in the bath, implying that the leak current is not abolished by the substrate. More importantly, DS reduces the current below control levels even in the absence of NE. We therefore write hNET current I_{total} as the sum of three components: transient current, substrate-induced current and substrate-independent leak current:

$$I_{total} = I_{transient} + I_{substrate} + I_{leak}. \quad (7)$$

Fig. 7A shows typical data before subtraction. The kinetics of the on-step is shown at higher resolution in the inset. CO indicates the control current of the transfected cell in response to a −120 mV step from a −40 mV holding potential (no substrate, no inhibitor). GU indicates that substrate was added (30 μmol l^{-1} GU, no inhibitor) and DS indicates that inhibitor was added (30 μmol l^{-1} GU, 1 μmol l^{-1} DS). GU − CO therefore represents (substrate, no inhibitor) − (no substrate, no inhibitor), and this effectively removes the rapid transient (Fig. 7B), resulting in an inward current that gradually approaches a steady state. This finding indicates that the transient current is not peculiar to hNET operating with the substrate GU, as it must have been present in the control current in order to have been subtracted. We fitted the GU-induced current with the equation:

$$I_{substrate} = I_{GU(-40)} + I_{GU(-120)}[1 - \exp(-t/\tau_{GU(-120)})], \quad (8)$$

where t is time (in s) and τ is the decay constant. This equation describes the GU-induced current at −120 mV, which reaches a steady-state I_{GU} when $t \gg \tau_{GU}$=12 ms. Fig. 7C illustrates CO − DS, representing (no substrate, no inhibitor) − (substrate, inhibitor). This isolates the steady-state leak current (see Fig. 3 for an example). Notice that CO − DS also reveals a rapidly decaying inward transient current. To remove the steady-state leak component, we have arbitrarily assumed that the leak current is described by a formula similar to that for the substrate-induced current:

$$I_{leak} = I_{l(-40)} + I_{l(-120)}[1 - \exp(-t/\tau_{l(-120)})], \quad (9)$$

which reaches a steady-state value I_l when $t \gg \tau_l$. We assumed that the time constant of the leak current is fast compared with that of the transient current. Using this equation, with τ_l between 1 and 2 ms, gave single-exponential fits to the transient decay. Merely subtracting the steady current $I_{l(-120)}$ gave double-exponential fits to the transient decay. We have not explored this further and have used the full equation for leak subtraction. Notice that $I_{l(-40)}$ is approximately zero, which indicates that the leak reversal potential is positive to −40 mV. We have verified this by extrapolation of $I_{leak}(V)$ plots in three experiments (data not shown). In Fig. 7D, we

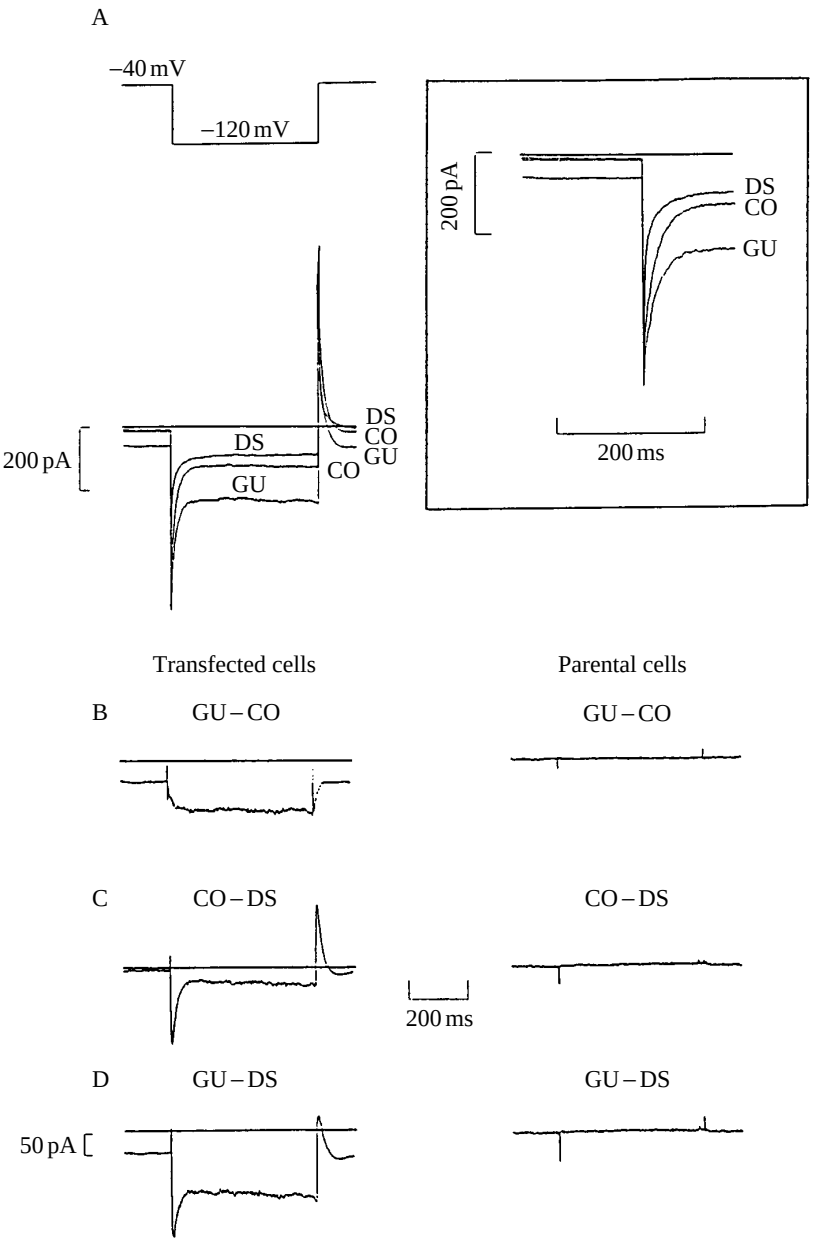

Fig. 7. Subtraction procedures reveal hNET-specific transient and steady-state currents. (A) Raw data before subtraction. In this typical experiment, the 293-hNET cell was held at −40 mV and stepped to −120 mV for 500 ms. Raw data and difference currents are analyzed without leak or capacitative compensation. The labels refer to: control current before adding substrate (CO), substrate-induced current after adding 30 μmol l^{-1} guanethidine to the bath (GU) and inhibited current after adding 1 μmol l^{-1} desipramine to the bath (DS, note that GU is still present). The inset shows the transient currents on an expanded time scale. (B) GU-induced current defined by control. GU induces an inward current at the holding potential (−40 mV) and the test potential (−120 mV). After a step from −40 to −120 mV, the GU-induced current, defined as (GU − CO), rises exponentially to a steady state with a time constant $\tau_{GU(-120)}$ of 12 ms. The panel on the right shows the same subtraction procedure performed on a parental cell. (C) DS-blocked current. Adding 2 μmol l^{-1} DS to the bath abolishes the GU-induced current and reveals a residual transient current and a steady-state leak current, defined by (CO − DS). The transient has a decay time constant $\tau_{t(-120)}$ of 12.5 ms. The panel on the right shows the same procedure performed on a parental cell. (D) GU-induced current defined by inhibitor. The GU-induced current, defined by (GU − DS), is the sum of the currents in B and C. The panel on the right shows the same procedure performed on a parental cell.

consider GU − DS derived from (substrate, no inhibitor) − (substrate, inhibitor). This is the total hNET-mediated current defined by the antagonist. It contains a rapid inward transient and a steady-state component composed of a substrate-induced current and a leak current. Using these empirical formulae, we define transporter-associated transient currents by (CO − DS) − I_{leak}. We described this transient by:

$$I_{transient} = I_{t(-120)}\exp(-t/\tau_{t(-120)}) . \quad (10)$$

The time constant for the transient current shown in Fig. 7 is $\tau_{t(-120)}$=12.5 ms.

Transient currents depend on voltage but not on amine substrate

Fig. 8A shows a family of leak-subtracted transient currents, (CO − DS) − I_{leak}, obtained from voltages between −60 and −140 mV. The experiments and subtractions were performed in 30 μmol l^{-1} GU and 2 μmol l^{-1} DS, implying full occupancy of the binding sites for substrate or inhibitor. Fig. 8B plots the area under the leak-subtracted transient currents *Q* as a function of voltage (normalized at −120 mV). Absolute values ranged from 1.19 to 5.60 pC (five cells). Fig. 8C shows a similar analysis without GU. *Q* in this case ranged from 0.54 to 7.1 pC (five cells). The time constant of the transient in NE or in GU varied from 5±3 ms at −60 mV to 11±5 ms at −140 mV. This analysis indicates that the size and the kinetics of the transient current depend on voltage; however, the charge movement associated with the transient is approximately the same with or without amine substrate.

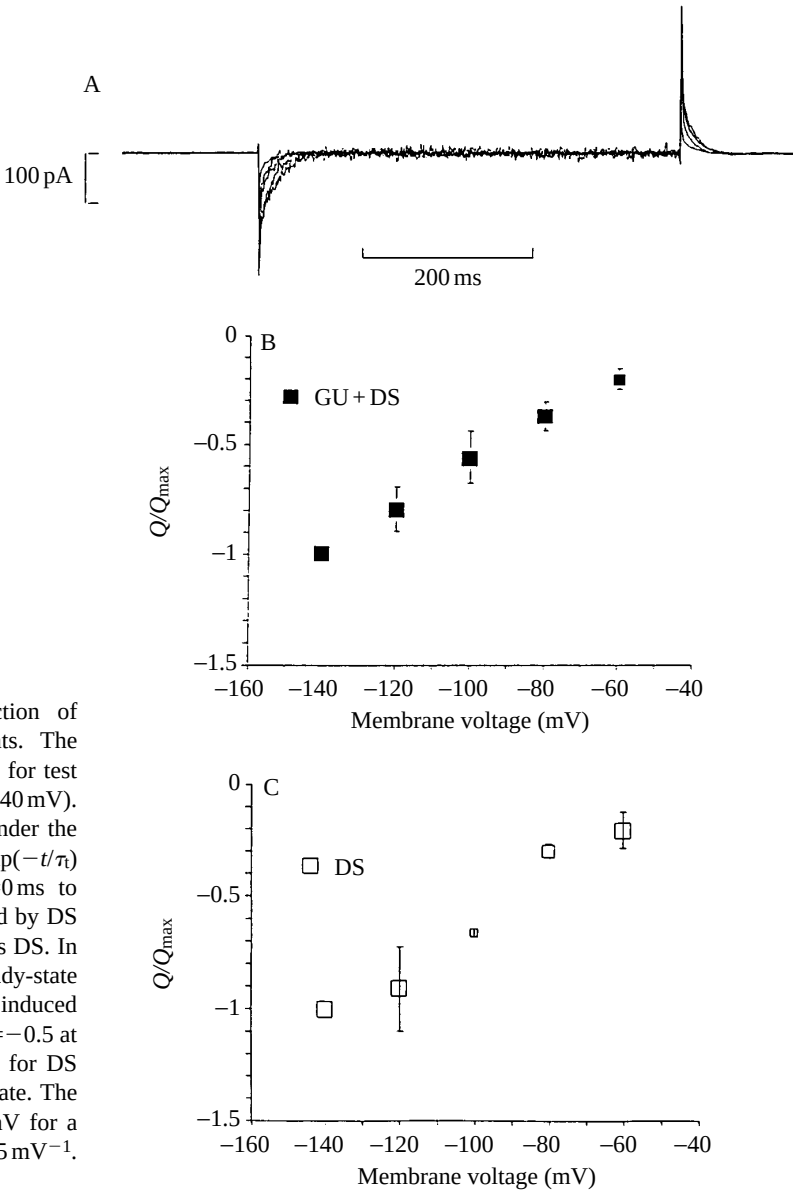

Fig. 8. Transient charge movement in hNETs as function of membrane voltage. (A) Leak-subtracted transient currents. The difference current (CO − DS) minus the leak current (I_{leak}) for test voltages between −60 and −140 mV (holding potential −40 mV). The transient charge (Q) was calculated from the area of under the leak-subtracted transients fit to the equations: $I_{transient}=I_t\exp(-t/\tau_t)$ and $Q=\sum[I_{transient}]dt$, where the integration Σ is from t=0 ms to t=200 ms, I_t is the amplitude of the transient current revealed by DS and τ_t is its decay constant. (B) Cumulative data for GU plus DS. In this protocol, 30 μmol l^{-1} GU was added to induce a steady-state current and then 2 μmol l^{-1} DS was added to block the induced current (average Q from five cells) at each potential. $Q/Q_{max}=-0.5$ at −93 mV and the slope=0.0105 mV^{-1}. (C) Cumulative data for DS only. In this protocol, we added DS in the absence of substrate. The Q values for B and C were normalized to Q_{max} at −140 mV for a given cell. $Q/Q_{max}=-0.5$ at −91 mV and the slope=0.0125 mV^{-1}. Values are means ± S.E.M., N=3.

Transient currents do not depend on external Na^+

Although the transient current does not depend on the amine substrate, it may represent the movement of Na^+ through the channel or off the binding site. To test this, we analyzed the transient current in the presence and absence of external Na^+. In the experiment shown in Fig. 9A, adding 15 μmol l^{-1} NE increased the steady-state current as previously described. Under constant perfusion, we substituted Li^+ for Na^+, resulting in a decrease of current below control levels. The fast inward transient, however, remains essentially unchanged after Li^+ substitution. The insets show raw data (top) and normalized data (bottom). Fig. 9B,C shows the difference currents (NE − CO) and (CO − No Na^+). These subtractions eliminate capacitance current. GU-induced currents generally appear to turn on more slowly than the NE-induced currents, but we have not studied this systematically. The transient current in the absence or presence of Na^+ is approximately the same. In marked contrast to (CO − DS) in Fig. 7, (CO − No Na^+) results only in a steady-state leak. It is possible that Li^+ binds tightly to the transporter with no change in intrinsic charge movement. We have carried out similar experiments using Tris as a substrate (TrisCl substituted for NaCl) with essentially the same result (N=5). In some experiments, a slight decrease in the transient occurs in (0 mmol l^{-1} Na^+)–Tris solutions; the decrease was far smaller than in (130 mmol l^{-1} Na^+)–DS solutions. Tris-substitution decreases the steady-state control current as expected, but leaves the transient current essentially unaltered. These experiments show that whereas Na^+ is essential for the steady-state current, it is not essential for the transient current revealed by DS block.

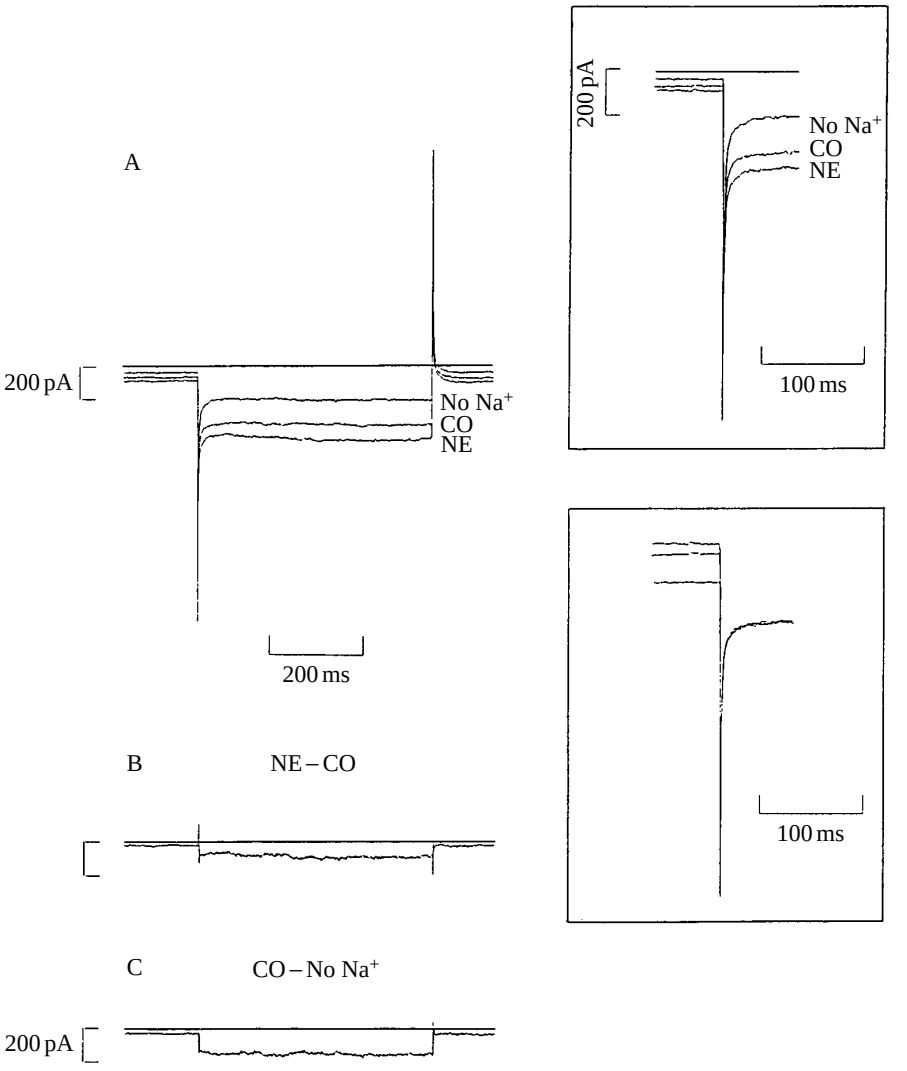

Fig. 9. Transient currents as a function of external [Na^+]. (A) Raw data before subtraction. In these experiments, the cell was held at −40 mV and stepped to −120 mV. Raw data and difference currents are analyzed without leak or capacity compensation. The labels refer to: control before adding substrate (CO), substrate-induced current after adding 15 μmol l^{-1} norepinephrine to the bath (NE) and inhibited current after perfusion with a Na^+-free solution (No Na^+, LiCl replacement). The insets show the transient currents on an expanded time scale. The top inset shows the raw data; the bottom inset shows the same data normalized at 75 ms into the test pulse. (B) NE-induced current defined by control. NE induces an inward current at both the holding potential (−40 mV) and the test potential (−120 mV). After a step from −40 to −120 mV, the NE-induced current, defined as (NE − CO), rises abruptly to a steady state without a transient current. (C) Na^+-blockable current. Removing Na^+ from the bath abolishes the NE-induced current and reveals a residual steady-state leak current defined by (CO − No Na^+). After a step from −40 to −120 mV, the leak current rises abruptly to a steady state without a transient current.

Discussion

In vitro flux assays suggest that the transport of NE into presynaptic terminals couples to the movement of Na^+ and Cl^- with a stoichiometry of $1NE^+$:$1Na^+$:$1Cl^-$ (Harder and Bönisch, 1985; Friedrich and Bönisch, 1986; Ramamoorthy *et al.* 1993*a*,*b*). Presumably, coupling occurs when the catecholamine substrate and the cotransported ions simultaneously occupy external binding sites on the NET protein. The loaded transporter then releases both its substrate and the cotransported ions into the cell and returns unoccupied sites to the external surface to begin a new cycle. Assuming the above stoichiometry, coupled transport would generate a depolarizing inward current of a size dictated by cycle time and the net charge of bound substrates. For this reason, NE uptake ought to depend on membrane voltage. In addition, voltage-dependence may result from conformational changes and translocation steps. Finally, ion pathways could open when amines or cotransported ions bind to hNET, introducing additional voltage-dependence of uncoupled ion flow. Until recently, the study of NE transport mediated by NETs has relied exclusively on radiolabeled uptake assays. These assays are carried out on populations of cells; thus, parameters that depend on membrane voltage are poorly defined. Furthermore, the voltage may change during the experiment. For these reasons, the voltage regulation of NE uptake, which is likely to be an important factor in the normal function of transporters, is largely unknown.

Re-sealed vesicles from PC-12 (pheochromocytoma) cells or placental brush-border cells are a more controlled alternative because they have fixed or imposed membrane potentials and ion gradients (Harder and Bönisch, 1985; Friedrich and Bönisch, 1986; Ramamoorthy *et al.* 1993*a*,*b*). These preparations support the claim that NE uptake is electrogenic and that uptake represents coupled transport with fixed stoichiometry. However, this method has poor temporal resolution and does not report ion flow, as distinct from ion dependence. Because some vesicles could be defective, estimates of transporter density or turnover contributing to transport may be deflated by non-functional carriers. Re-sealed vesicles have small volumes, and their kinetic parameters may be contaminated by intracellular filling. These problems are alleviated for transporters under voltage control with

intracellular volumes connected to a diffusion pathway, as in whole-cell voltage-clamp studies.

We have constructed a stable cell line (293-hNET) from HEK-293 cells transfected with a single species of human NET cDNA. These cells have an uptake profile and pharmacology associated with NETs: (a) 293-hNET cells saturate at submicromolar concentrations of NE (K_m=420 nmol l^{-1}) with a Hill coefficient near unity; (b) selective antagonists, such as desipramine and nomifensine, block NE uptake at concentrations that conform to published values; (c) maximum uptake velocity is similar to that of other expression systems; (d) the radiolabeled NET antagonist RTI-55 binds hNET-293 membranes with appropriate affinity. Transport turnover rates estimated from radiolabeled flux and binding data are 2–3 NE$^+$ s^{-1} (Bönisch and Harder, 1986). This agrees with our uptake and binding data which, from V_{max} and B_{max}, yield a cycle rate of 1.7 s^{-1}. Qualitatively similar results were obtained with different independent clones of our stable transformation, indicating no relationship with chromosomal integration sites. At the assumed stoichiometry, these rates predict approximately 0.1 pA per cell for 10^6 transporters. In contrast to this discouragingly low prediction, we can readily observe −50 pA of NE-induced current at −120 mV. Furthermore, other neurotransmitter transporters for glutamate, GABA and serotonin can generate 100 pA of inward current or more from a single cell held at negative potentials (Brew and Atwell, 1987; Schwartz and Tachibana, 1989; Schwartz, 1982, 1987; Risso *et al.* 1992; Bruns *et al.* 1993; Risso *et al.* 1992). In addition, GABA and serotonin transporters expressed in *Xenopus laevis* oocytes yield comparable currents when scaled for surface area (Mager *et al.* 1993, 1994; Lester *et al.* 1994). Thus, the amine-induced currents in 293-hNET cells, while much larger than expected from V_{max} and B_{max} assuming coupled transport theory, are nevertheless in line with neurotransmitter-induced currents measured in other preparations.

At saturating concentrations, NE induces a nominal −50 pA at −120 mV in transfected cells. This extrapolates to −15 pA at a resting potential of −40 mV, many times greater than expected even assuming that all NETs measured by radioligand binding are on the surface. One explanation for the large currents might be turnover rates that are much higher than we estimated. At the assumed stoichiometry, 15 pA would require 10^6 transporters turning over in 100 s. Accumulated radioactivity could reach a plateau at incubation times much shorter than 10 min, leading to an underestimate of turnover rate. To control for this possibility, we have repeated our studies using saturated concentrations of NE and find that rates equivalent to those reported (within ±10 %) down to 10 s. Thus, as nearly as we can measure, radioligand uptake predicts a turnover rate of 1.7 s^{-1}, at variance with the NE-induced current from similar cells. Thus, we were led to seek other explanations for these data. Another interpretation of these large currents is that hNET introduces NE- and Na$^+$-dependent uncoupled current of indefinite stoichiometry. This mechanism has already been suggested for the serotonin (5-HT) and GAT1 transporters (Lester *et al.* 1994; Cammack *et al.* 1994). For example, Mager *et al.* (1994) show that whereas 5-HT transport in *Xenopus laevis* oocytes compares with vesicle studies (Rudnick and Clark, 1993), the 5-HT-induced currents are nearly 10 times larger than predicted by coupled 1 5-HT:1Na$^+$:1Cl$^-$ transport.

One way to introduce uncoupled transport is to visualize hNETs as both amine carriers and ligand-gated channels. In this view, NE and Na$^+$ (and possibly Cl$^-$) act as ligands that open a gate, allowing ions through the transporter. An important difference is that, unlike a classical ligand-gated channel, the ligands themselves are also transported. Furthermore, even though currents from populations of transporters may be significant, transporter channels may have orders-of-magnitude smaller conductance than ligand-gated channels. Transporter channels, if they exist, have unusual properties. NE- and Na$^+$-induced currents obey Michaelis–Menten kinetics; however, they bind with very different affinities (50 % activity at saturating [Na$^+$] requires 520 nmol l^{-1} NE, whereas 50 % activity at saturating NE requires 15 mmol l^{-1} Na$^+$). Moreover, although substrates such as GU can substitute for NE, Li$^+$ cannot substitute for Na$^+$. No homology has been revealed between Na$^+$-dependent cotransporters and ligand-gated channels, suggesting convergent rather than homologous permeation mechanisms.

Although NE- and GU-induced currents follow similar Michaelis–Menten kinetics, GU-induced currents are more than twice the magnitude under comparable conditions. At pH 7.4, the charge on GU should be about +3e$^-$, which might account for the bigger current. However, further studies in which GU and NE are applied to the same cell should help to address this issue. Regardless of the differences in absolute magnitude, the $I(V)$ curves generated by NE and GU have the same voltage-dependence between −40 and −140 mV. Thus, the voltage-dependent mechanism appears to be independent of the charge on the amine substrate. This appears to be counterintuitive if GU binds in the electric field of the membrane and suggests that voltage-dependence reflects the driving force of amine-dependent, uncoupled flow of ions.

Desipramine, a highly specific antidepressant for NETs (Pacholczyk *et al.* 1991; Barker and Blakely, 1995), inhibits the uptake of NE in flux assays and it blocks the NE-induced current in voltage-clamp experiments. It turns out that DS blocks not only substrate-induced current but also a fraction of the control current (no substrate or inhibitor). This observation was puzzling at first, because it implied a non-specific action of DS on HEK-293 cells. However, DS has no effect on non-transfected cells, and the leak current is associated exclusively with the transporter. Stated in another way, the transporter itself, even in the absence of substrate, introduces a conductance pathway into the membrane. A similar leak has been reported in Na$^+$/glucose transporters and in GABA transporters (Parent *et al.* 1992; Mager *et al.* 1993). Although we have not methodically studied the reversal potential of the leak current, it is approximately −40 mV. In 10 μmol l^{-1} DS or 10 μmol l^{-1} cocaine, the average leak is less than 10 % of

the total induced current, although in an individual cell it can be as large as 30 %. Higher concentrations of cocaine reveal an average leak as large as 40 % of induced current. These high-dose effects probably include non-specific actions of cocaine.

Desipramine also reveals a transient current that is absent in parental cells. The hNET-associated transient occurs immediately after a hyperpolarizing step and decays with a time constant similar to that of the steady-state current. DS blocks the steady-state and the transient (pre-steady-state) currents. The charge under the transient current, $Q(V)$, ranged from nominal values of 1 pC at −60 mV to 5 pC at −120 mV in a nearly linear relationship. $Q(V)$ was approximately the same whether or not we had previously added substrate. This implies that the charge movement is independent of the substrate and is associated either with the transporter itself or with a cotransported ion. In the range we studied, $Q(V)$ does not show the clear saturation seen in the Na^+/K^+ pump and in GABA transporters (Nakao and Gadsby, 1986; Mager *et al.* 1993). In Fig. 8C, however, the data appear to be approaching saturation. Assuming movement of one charge across the field, a nominal displacement of 5 pC implies about 3×10^7 hNETs per cell. For Na^+/K^+ pumps operating as Na^+/Na^+ exchangers (Nakao and Gadsby, 1986; Gadsby *et al*. 1993), the movable charge was 3.9 pC. Although comparable to our value, the myocytes were larger than our cells (approximately 180 pF). Furthermore, the density of Na^+/K^+ pumps in cardiac cells is high (approximately 1000 μm^{-2}) and the pump current (5.4 mmol l^{-1} external K^+, 50 mmol l^{-1} internal Na^+ and 10 mmol l^{-1} internal ATP) was approximately 200 pA. These values gave a turnover rate, I_{max}/Q_{max}, of 50 s^{-1}. 293-hNET $I(V)$ curves do not show convincing saturation at either end of the voltage range we tested; however, at −120 mV at saturating concentrations, the I/Q ratio yields a turnover rate for hNET of 20 s^{-1}. The number of transporters calculated from Q is 10 times that determined by ligand binding. It is possible that we selected cells with unusually high densities; however, we suspect that charge movement in 293-hNET cells reflects more than $1e^-$ per transporter and may not represent charge moving through the transporter channel.

Mager *et al.* (1993) show that, in the absence of GABA, voltage jumps produce charge movements that are suppressed by SKF-89976A. GABA-induced currents depend absolutely on external Na^+, and transients in low $[Na^+]$ shifted the charge movement to more negative voltages. At 10 mmol l^{-1} $[Na^+]_o$ the curve shifted to −140 mV, and in zero $[Na^+]_o$ there was no transporter charge movement. Cammack *et al.* (1994) investigated the GAT1 transient in stably transfected HEK-293 cells. In this case, the transient required external Na^+, and they concluded that transients do not reflect internal movement of transporter charge. To test whether Na^+ plays a role in hNET $Q(V)$ curves, we replaced Na^+ with Li^+. In these experiments, it was not possible to perform DS subtractions in the absence of Na^+ because DS binding is Na^+-dependent (Böndish and Harder, 1986). Although Li^+ substitution had no effect on the transient current, Li^+ may recognize the Na^+ binding site. To test this, we replaced Na^+ by Tris, assuming that it is unlikely that Tris would bind to the Na^+ site. However, Tris replacement gave the same result as Li^+ replacement. From these experiments, we conclude that Na^+ does not contribute to the transient current. Because neither amine substrate nor Na^+ contributes to the transient, we tentatively conclude that the pre-steady-state currents result from internal movement of charge confined to the membrane and localized to the transporter. It is possible that apparent charge movement may involve the loading and unloading of Cl^-. Further experiments are required to separate intrinsic charge movements from ions driven off by voltage jumps.

In summary, we have established a stable hNET-expressing mammalian cell line suitable for patch-clamp analyses of catecholamine transporters. Using this line, we demonstrate that heterologous expression of hNETs results in catecholamine translocation and net current. The dependence of the steady-state currents on amine substrate and Na^+ are consistent with coupling models of a $1Na^+$:$1Cl^-$:1NE stoichiometry. hNET also mediates constitutively gated ion flow (the so-called leak current). The magnitude of the NE-gated current relative to the transporter density suggests either (1) a much higher turnover rate than has previously been proposed or, (2) the existence of a major amine-gated, but uncoupled, ion channel pathway within the transporter. We thus propose a model in which NETs bind specific substrates and ions with definite stoichiometry and that this binding initiates the translocation of amines. However, this binding may, on occasion, open a parallel pathway for the movement of charge through the transporter. In other words, we believe that – in addition to the more traditional mode associated with the coupled translocation of neurotransmitter – NETs contain modes of conduction that correspond to ligand-gated ion channels. At present we do not know the relative frequency of the two modes of operation. This awaits direct measurements of the single-channel events, which are now under way in our laboratory. Finally, we note that the hNET transient current relaxes with a time constant quite similar to that of the onset of the amine-dependent steady-state current, suggesting to us that the transient current may reflect the movement of an intrinsic charge linked to the opening of the transporter's ion-conducting pathway. Unlike the steady-state current, which is abolished by Li^+ or Tris replacement of Na^+, the transient current apparently functions without Na^+. This implies that the transient current does not solely represent the unbinding of bound alkali metal as a transition to the open state.

We thank Haley Melikian for assistance with Western blots, Fernanda Laezza for data on the Na^+-dependence of the GU-induced currents, Joseph Justice for the donation of cocaine, F. Ivy Carrol for unlabeled RTI-55 and Gary Rudnick for LLC-NET cells. This research was supported by NIH HL-27388 and University Research Grant 2-50763 to L.J.D. and NIH grants NS-33373 and DA-07390 and a Mallinckrodt Award to R.D.B. The authors wish to thank Criss Hartzell for useful suggestions

during various stages of this research and Alex Daniels and Bill Goolsby for computer and electronics support.

References

AMARA, S. AND KUHAR, M. J. (1993). Neurotransmitter transporters: recent progress. *A. Rev. Neurosci.* **16**, 73–93.

ATWELL, D., BARBOUR, B. AND SZATKOWSKI, S. (1993). Nonvesicular release of neurotransmitter. *Neuron* **11**, 401–407.

AXELROD, J. (1971). Noradrenaline: fate and control of its biosynthesis. *Science* **173**, 598–603.

AXELROD, J., WHITBY, L. G. AND HERTTING, G. (1961). Effect of psychotropic drugs on uptake of [^{3}H]norepinephrine by tissues. *Science* **133**, 383–384.

BARKER, E. AND BLAKELY, R. D. (1995). Antidepressant-sensitive norepinephrine and serotonin transporters. In *Psychopharmacology*: *The Fourth Generation of Progress* (ed. F. E. Bloom and D. J. Kupfer). New York: Raven Press (in press).

BERNATH, S. (1991). Ca-independent release of amino acid neurotransmitter: fact or fiction? *Prog. Neurobiol.* **38**, 57–91.

BLAKELY, R. D. (1993). Advances in molecular biology of neurotransmitter transporters. *Curr. Opin. Psychiat.* **5**, 69–73.

BLAKELY, R. D., BERSON, H. E. AND FREMEAU, R. T. (1991*a*). Cloning expression of a functional serotonin transporter from rat brain. *Nature* **354**, 66–70.

BLAKELY, R. D., CLARK, J. A. AND RUDNICK, G. (1991*b*). Vaccinia–T7 RNA polymerase expression systems: evaluation for the expression cloning of plasma membrane transporters. *Analyt. Biochem.* **194**, 302–308.

BLAKELY, R. D., DEFELICE, L. J. AND HARTZELL, H. C. (1994). Molecular physiology of norepinephrine and serotonin transporters. *J. exp. Biol*. **196**, 263–281.

BOGDANSKI, D. F. AND BRODIE, B. B. (1966). Role of sodium and potassium ions in storage of norepinephrine by sympathetic nerve endings. *Life Sci.* **5**, 1563–1569.

BÖNISCH, H. AND HARDER, R. (1986). Binding of ^{3}H-desipramine to the neuronal NE carrier of rat PC-12 cells. *Archs Pharmac.* **334**, 403–411.

BREW, H. AND ATTWELL, D. (1987). Electrogenic glutamate uptake is a major current carrier in the membrane of axolotl retinal cells. *Nature* **327**, 707–710.

BRUNS, K. J., ENGERT, F. AND LUX, H. D. (1993). A fast activating presynapse reuptake current during serotonergic transmission in identified neurons of *Hirudo*. *Neuron* **10**, 559–572.

CAMMACK, J. N., RAKHILIN, S. V. AND SCHWARTZ, E. A. (1994). A GABA transporter operates asymmetrically with variable stoichiometry. *Neuron* **13**, 949–960.

CHENG, Y.-C. AND PRUSOFF, W. H. (1973). Relationship between the inhibition constant (K_i) the concentration of an inhibitor which causes 50 per cent inhibition (I_{50}) of an enzymatic reaction. *Biochem. Pharmac.* **22**, 3309–3108.

CLARK, J. A., DEUTCH, A. Y., GALLIPOLI, P. Z. AND AMARA, S. G. (1992). Functional expression CNS distribution of a β-alanine-sensitive neuronal GABA transporter. *Neuron* **9**, 337–348.

CLARKSON, C. W. AND OTHERS (1993). Electrophysiological effects of high cocaine concentrations on intact canine heart: Evidence for modulation by both heart rate autonomic nervous system. *Circulation* **87**, 950–962.

FRIEDRICH, U. AND BÖNISCH, H. (1986). The neuronal NET system of PC-12 cells: kinetic analysis of the interaction between NE:Na:Cl transport. *Archs Pharmac.* **333**, 246–252.

FUERST, T. R., NILES, E. G., STUDIER, F. W. AND MOSS, B. (1986). Eukaryotic transient expression system based on recombinant vaccinia virus that synthesizes bacteriophage T7 RNA polymerase. *Proc. natn. Acad. Sci. U.S.A.* **83**, 8122–8126.

GADSBY, D. C. AND NAKAO, M. (1989). Steady-state current–voltage relationship of the Na/K pump in guinea pig ventricular myocytes. *J. gen. Physiol*. **94**, 511–537.

GADSBY, D. C., RAKOWSKI, R. F. AND DE WEER, P. (1993). Extracellular access to the Na, K pump: pathway similar to ion channels. *Science* **260**, 100–103.

GANGULY, P. K., DHALLA, K. S., INNES, I. R., BEAMISH, R. E. AND DHALLA, N. S. (1986). Altered NE turnover and metabolism in diabetic cardiomyopathy. *Circulation Res.* **59**, 684–693.

GLASSMAN, A. H., ROOSE, S. P., GIARDINA, E.-G. AND BIGGER, J. T., JR (1985). Cardiovascular effects of tricyclic antidepressants. In *Psychopharmacology: The Third Generation of Progress* (ed. H. Y. Meltzer). New York: Raven Press.

GONON, F., BAO, J. X., MSGHINA, M., SUAUD-CHAGNY, M. F. AND STJÄRNE, L. (1993). Fast and local electrochemical monitoring of noradrenaline release from sympathetic terminals in isolated rat tail artery. *J. Neurochem.* **60**, 1251–1257.

GU, H., WALL, S. C. AND RUDNICK, G. (1994). Stable expression of biogenic amine transporters reveals differences in inhibitor sensitivity, kinetics and ion dependence. *J. biol. Chem*. **269**, 7124–7130.

HARDER, R. AND BÖNISCH, H. (1985). Effects of monovalent ions on the transport of NE across the plasma membrane of neuronal cells (PC-12 cells). *J. Neurochem.* **45**, 1154–1162.

HERTTING, G., AXELROD, J., KOPIN, I. J. AND WHITBY, L. G. (1961). Lack of uptake of catecholamines after chronic denervation of sympathetic nerves. *Nature* **189**, 66.

HOFFMAN, B. J., MEZY, E. AND BROWNSTEIN, M. J. (1991). Cloning of a serotonin transporter affected by antidepressants. *Science* **254**, 579–580.

IVERSEN, L. L. (1975). Uptake processes for biogenic amines. In *Handbook of Psychopharmacology* (ed. L. L. Iversen). New York: Plenum Press.

IVERSEN, L. L. AND KRAVITZ, E. A. (1966). Na dependence of transmitter uptake at adrenergic nerve terminals. *Molec. Pharmac.* **2**, 360–362.

KANNER, B. I. AND SCHULDINGER, S. (1987). Mechanism of transport and storage of neurotransmitters. *CRC Crit. Rev. Biochem*. **22**, 1–38.

KAPLAN, J. H. (1993). Molecular biology of carrier proteins. *Cell* **72**, 13–18.

LAUGER, P. (1991). *Electrogenic Ion Pumps.* MA: Sinauer Associates.

LESTER, H. A., MAGER, S., QUICK, M. W. AND COREY, J. L. (1994). Permeation properties of neurotransmitter transporters. *A. Rev. Pharmac. Toxicol*. **34**, 219–249.

MAGER, S., MIN, C., HENRY, D., CHAVKIN, C., HOFFMAN, B., DAVIDSON, N. AND LESTER, H. A. (1994). Conducting states of a mammalian 5HT transporter. *Neuron* **12**, 11–20.

MAGER, S., NAEVE, J., QUICK, M., GUASTELLA, J., DAVIDSON, N. AND LESTER, H. A. (1993). Steady states, charge movements, rates for a cloned GABA transporter expressed in *Xenopus* oocytes. *Neuron* **10**, 177–188.

MALCHOW, R. P. AND RIPPS, H. (1990). Effects of γ-aminobutyric acid on skate retinal horizontal cells: Evidence for an electrogenic uptake mechanism. *Proc. natn. Acad. Sci. U.S.A.* **87**, 8945–8949.

MELIKIAN, H. E., MCDONALD, J. K., GU, H., RUDNICK, G., MOORE, K. R. AND BLAKELY, R. D. (1994). Human norepinephrine transporter:

Biosynthetic studies using a site-directed polyclonal antibody. *J. biol. Chem.* **269**, 12290–12297.

NAKAO, M. AND GADSBY, D. C. (1986). Voltage dependence of a Na translocation by the Na/K pump. *Nature* **323**, 628–630.

PACHOLCZYK, T., BLAKELY, R. D. AND AMARA, S. G. (1991). Expression cloning of a cocaine-antidepressant-sensitive human noradrenaline transporter. *Nature* **350**, 350–354.

PALIJ, P. AND STAMFORD, J. A. (1992). Real-time monitoring of endogenous noradrenaline release in rat brain slices using fast cyclic voltammetry. I. Characterization of evoked noradrenaline efflux uptake from nerve terminals in the bed nucleus of the stria terminalis, pars ventralis. *Brain Res.* **587**, 137–146.

PARENT, L., SUPPLISSON, S., LOO, D. AND WRIGHT, E. M. (1992). Electrogenic properties of the cloned Na/glucose cotransporter I. *J. Membr. Biol.* **125**, 49–62.

RAMAMOORTHY, S., BAUMAN, A. L. AND MOORE, K. R. (1993*a*). Anti-depressant-cocaine-sensitive hSERT: molecular cloning, expression, chromosomal localization. *Proc. natn. Acad. Sci. U.S.A.* **90**, 2542–2546.

RAMAMOORTHY, S., PRASAD, P., KULANTHAIVEL, P., LEIBACH, F. H., BLAKELY, R. D. AND GANAPATHY, V. (1993*b*). Expression of a cocaine-sensitive norepinephrine transporter in the human placental syncitiotrophoblast. *Biochemistry, N.Y.* **32**, 1346–1353.

RISSO, R., DEFELICE, L. J. AND BLAKELY, R. D. (1992). Whole-cell analysis of electrogenic neurotransmitter transport in transfected HeLa cells. *J. gen. Physiol.* **100**, 43A.

RISSO, S., DEFELICE, L. J. AND BLAKELY, R. D. (1995). Na-dependent GABA-induced currents in GAT1-transfected HeLa cells. *J. Physiol., Lond.* (in press).

ROSS, S. B. (1987). Pharmacological toxicological exploitation of amine transporters. *Trends pharmac. Sci.* **8**, 227–231.

RUDNICK, G. AND CLARK, J. (1993). From synapse to vesicle: the reuptake storage of biogenic amine neurotransmitters. *Biochim. biophys. Acta Bio-energetics* **1144**, 249–263.

SAMMET, S. AND GRAEFE, K. H. (1979). Kinetic analysis of the interaction between NE and Na in neuronal uptake. *Archs Pharmac.* **309**, 99–107.

SANCHEZ-ARMÁSS, S. AND ORREGO, F. (1977). A major role for Cl in [^{3}H] noradrenaline transport by rat heart adrenergic nerves. *Life Sci.* **20**, 1829–1838.

SCHÖMIG, E., FISCHER, P., SCHONFELD, C.-L. AND TRENDELENBURG, U. (1989). The extent of neuronal reuptake of ^{3}H-noradrenaline in isolated vasa deferentia atria of the rat. *Archs Pharmac.* **340**, 502–508.

SCHÖMIG, A., HAASS, M. AND RICHARDT, G. (1991). Catecholamine release arrhythmias in acute myocardial ischaemia. *Eur. Heart J.* **12** (Suppl. F), 38–47.

SCHWARTZ, E. A. (1982). Calcium-independent release of GABA in isolated horizontal cells of the toad retina. *J. Physiol., Lond.* **323**, 211–227.

SCHWARTZ, E. A. (1987). Depolarization without calcium can release γ-aminobutyric acid from a retinal neuron. *Science* **238**, 350–354.

SCHWARTZ, E. A. AND TACHIBANA, M. (1989). Electrophysiology of glutamate Na cotransport in a glial cell of the salamander retina. *J. Physiol., Lond.* **426**, 43–80.

SMETS, L. A., BOUT, B. AND WISSE, J. (1988). Cytotoxic antitumor effects of the norepinephrine analogue meta-iodo-benzylguanidine (MIBG). *Cancer Chemother. Pharmac.* **21**, 9–13.

STEIN, W. D. (1986). *Transport Diffusion across Cell Membranes.* New York: Academic Press.

TRENDELENBURG, U. (1991). Functional aspects of the neuronal uptake of NE. *Trends pharmac. Sci.* **12**, 334–337.

WEIR, W. G. AND BEUCKELMANN, D. J. (1989). Na–Ca exchange in mammalian heart: I(V) relation and dependence on intracellular Ca concentration. *Molec. cell. Biochem.* **89**, 97–102.

WHITBY, L. G. AND AXELROD, J. (1961). The fate of ^{3}H-NE in animals. *J. Pharmac. exp. Ther.* **132**, 193–201.